Cancer Biomarkers 39 (2024) 1–13
DOI 10.3233/CBM-220410
IOS Press

circ_0058063 promotes breast cancer progression by upregulating DLGAP5 via sponging miR-557

Kongjun Zhu[a,1], Cen Yi[b,1] and Chuanming Tong[c,*]
[a]*Department of Thyroid and Breast Surgery, Wuhan NO.1 Hospital, Wuhan, Hubei, China*
[b]*Clinical Laboratory, Wuhan NO.1 Hospital, Wuhan, Hubei, China*
[c]*Department of General Surgery, People's Hospital of Dongxihu District, Wuhan, Hubei, China*

Received 8 November 2022
Accepted 22 May 2023

Abstract.
OBJECTIVE: Accumulating evidence indicates that circular RNAs (circRNAs) contribute to breast cancer (BC) development and progression. However, the role of circ_0058063 in BC and its underlying molecular processes remain unclear.
METHODS: The expression of circ_0058063, miR-557, and DLGAP5 in BC tissues and cells was determined using real time quantitative PCR or western blotting. The functions of circ_0058063 in BC cells were detected using CCK-8, Transwell, caspase-3 activity, and xenograft tumor assays. The specific binding of circ_0058063/miR-557 and DLGAP5/miR-557 was verified using RNA immunoprecipitation (RIP) and dual-luciferase reporter assays.
RESULTS: circ_0058063 expression was upregulated in BC tissues and cells. circ_0058063 knockdown inhibited proliferation and migration but promoted apoptosis in MCF-7 and MDA-MB-231 cells *in vitro*. *In vivo* studies further validated that the knockdown of circ_0058063 repressed tumor growth. Mechanistically, circ_0058063 directly sponged miR-557 and negatively regulated its expression. Additionally, miR-557 inhibition reversed the tumor-suppressive effects of the circ_0058063 knockdown on the survival of MDA-MB-231 and MCF-7 cells. Moreover, miR-557 directly targeted DLGAP5. DLGAP5 knockdown suppressed MCF-7 and MDA-MB-231 cell growth, and these effects were reversed by miR-557 downregulation.
CONCLUSION: Our findings verify that circ_0058063 acts as a sponge for miR-557 to upregulate DLGAP5 expression. These findings suggest that the circ_0058063/miR-557/DLGAP5 axis is an important regulator of oncogenic function and may be a promising therapeutic target for BC.

Keywords: circ_0058063, miR-557, DLGAP5, breast cancer

1. Introduction

Among all non-skin cancers, breast cancer (BC) has become the most common since 2004 [1,2]. Worldwide, approximately 30% of females are diagnosed with BC, with a mortality-to-incidence ratio of 15% [2]. Although the mortality rate has declined owing to improved techniques for early detection and effective systematic treatment, BC continues to be the most frequent type of cancer worldwide that causes death in women [3]. Early diagnosis and feasible targeted therapies are vital for patients with BC [4]. Therefore, the decline in BC mortality can be accelerated by exploring novel therapeutic targets and strategies.

In addition to being genetic, cancer is also epigenetic [5]. Approximately 10% of all BC cases are related to genetics [6]. Epigenetic mechanisms play vi-

[1]These authors contribute equally to this work.
*Corresponding author: Chuanming Tong, Department of General Surgery, People's Hospital of Dongxihu District, Intersection of the west side of Linkongang Avenue and the south side of Sandian Avenue, Dongxihu District, Wuhan 430040, Hubei, China. Tel./Fax: +86 15327362565; E-mail: chuanmingtong@163.com.

tal roles in regulating cancer progression and metastasis [7]. Prognostic and diagnostic tools based on epigenetics will significantly improve the precision of oncology [7]. Circular RNAs (circRNAs), discovered in the 1970s, have been recognized as a novel class of RNA that are widely found in various species [8]. When pre-mRNA is backspliced without the 3' tails and also 5' caps, single-stranded circular transcripts (circRNAs) are produced [9]. circRNAs are resistant to degradation and their expression is tightly regulated by RNA-binding proteins [9]. Notably, circRNAs can serve as miRNA sponges, templates for protein translation, RNA-binding protein scaffolds, or transcriptional regulators [10]. Recent research has demonstrated that circRNAs are dynamically produced in cancer and are essential components of epigenetic regulatory pathways in tumor growth [11]. Therefore, as research on tumor circRNAs has increased, circRNAs may now be used as unique potential biomarkers for the detection and management of various cancers.

Accumulating evidence has shown that circRNAs are dysregulated and contribute to the development of various cancers [12–14]. CircRNAs, such as circ-RPPH1, circ 0000514, circBCBM1, and cirCHIPK3, have been found to have strong potential for controlling cell migration, tumor growth, proliferation, and metabolism in BC. Their expression is also associated with prognosis and tumor node metastasis (TNM) stages [15–18]. However, the biological function of most circRNAs in BC remains largely unknown. According to previous reports, circ_0058063 is overexpressed and has an oncogenic function in a number of cancer types, suggesting that circ_0058063 may contribute to certain malignancies [19,20]. However, its role in BC has not yet been elucidated.

In this study, circ_0058063 was the primary focus, and its biological properties as well as the underlying molecular processes in BC formation were investigated. Our findings suggest that targeting the circ_0058063/miR-557/DLGAP5 axis may be a novel strategy for the treatment of BC.

2. Materials and methods

2.1. Human samples collection

Informed consent was obtained from 36 patients with BC who underwent surgery and the associated neighboring normal breast tissues were collected. No radiation or chemotherapy was administered to any patient before surgery. All tissues were placed in liquid nitrogen immediately and then stored at -80°C for further detection. The tissue samples were verified by two experienced pathologists. This study was approved by the Ethics Committee of our hospital. The Declaration of Helsinki and its revisions were followed for all procedures involving human participants. Table 1 lists the clinical characteristics of patients with breast cancer.

Table 1
The clinical characteristics of patients with breast cancer

Characteristics	Cases ($n = 36$)
Age	
$\geqslant 55$	18
< 55	18
Histologic grade	
I	7
II	19
III	10
Lymph node metastasis	
No	21
Yes	15
ER	
Negative	12
Positive	24
PR	
Negative	16
Positive	20
HER2	
Negative	21
Positive	15
Molecular subtype	
TNBC	11
Non-TNBC	25

TNBC, Triple-negative breast cancer.

2.2. Cell culture

The cell lines included a normal breast cell line (MCF-10A, cat, no. BNCC337734) and two BC cell lines (MDA-MB-231, cat. no. BNCC337894; MDA-MB-468, cat.no. BNCC339862) obtained from BeNa Culture Collection (Beijing, China). The remaining MCF-7 BC cells (cat. no. ZY-H061) were purchased from Ze-Ye Biotechnology Co., Ltd. (Shanghai, China). Dulbecco's Modified Eagle's Medium (DMEM; Invitrogen, USA) supplemented with 10% fetal bovine serum was used to cultivate all of the aforementioned cells (FBS; Gibco, USA). At 37°C, all cells were grown and incubated in a 5% CO_2 environment. The cells were trypsinized and passaged at a ratio of 1:3 until they reached 80% confluence.

2.3. Cell transfection

Non-targeting siRNA (Si-NC), siRNA targeting circ_0058063 or DLGAP5 (Si-circ or Si-DLGAP5),

Table 2
Real-time PCR Primer synthesis list

Name	Primer	Sequence
circ_0058063	Forward primer	5'-CAGCTCTGATGCCTTCTTCC-3'
	Reverse primer	5'-GGAAGCGACCAGATTCAAAC-3'
miR-557	Forward primer	5'-GTTTGCACGGGTGGGCC-3'
	Reverse primer	5'-CAGTGCGTGTCGTGGA-3'
DLGAP5	Forward primer	5'-CATCTGGAATGTCCAATTCAAG-3'
	Reverse primer	5'-ATGAAGGTCGAATT GCTCAG-3'
ATIC	Forward primer	5'-CACGCTCGAGTGACAGTG- 3'
	Reverse primer	5'-TCGGAGCTCTGCATCTCCG- 3'
U6	Forward primer	5'-CTCGCTTCGGCAGCACA -3'
	Reverse primer	5'-AACGCTTCACGAATTTGCGT -3'
GAPDH	Forward primer	5'-GTCTCCTCTGACTTCAACAGCG -3'
	Reverse primer	5'-ACCACCCTGTTGCTGTAGCCAA-3'

miR-557 overexpression plasmid (miR-557 mimic:5'-GUUUGCACGGGUGGGCCUUGUCU-3') or miR-NC, miR-557 knockdown plasmid (miR-557 inhibitor: 5'-AGACAAGGCCCACCCGUGCAAAC-3') or inhibitor control (inhibitor-NC) were purchased from Ruibo (Shanghai, China). 24-well plates with 5×10^4 MCF-7 as well as MDA-MB-231 cells each were seeded and cultured overnight. These cells were transfected with Si-NC, Si-circ, Si-DLGAP5, miR-557 mimic, miR-NC, miR-557 inhibitor, or NC inhibitor using the Lipofectamine 3000 transfection reagent (Invitrogen, Carlsbad, CA, USA) following the manufacturer's instructions. After incubation for 48 h, the transfection efficiency was determined by western blotting or real time quantitative PCR (RT-qPCR).

2.4. RT-qPCR

Total cellular RNA was extracted from lncRNA/mRNA using RNAiso Plus (TaKaRa Biotechnology, Japan). RNA was converted into cDNA using the First Strand cDNA Synthesis Kit (Thermo Scientific, USA). Using the Eco RT-PCR System, specific cDNAs was amplified with iTaqTM Universal SYBR® Green (Bio-Rad, USA). lncRNA and mRNA levels were measured using GAPDH as an internal reference. In addition, miRNAs were isolated using an miRNA isolation kit (OMEGA) and transcribed using the miRcute Plus miRNA First-Strand cDNA Synthesis Kit (TIANGEN, China). TIANGEN (Illumina, China) supplied the miRcute miRNA qPCR detection kit (SYBR Green) and Eco real-time PCR equipment for cDNA amplification. U6 served as the internal miRNA control. 95°C for 2 minutes, followed by 40 cycles of 95°C for 5 s and 60°C for 30 s, were the reaction conditions. The $2^{-\Delta\Delta CT}$ relative quantitative technique was used to examine target gene expression. The primer sequences are listed in Table 2.

2.5. Subcellular fractionation location

Nuclear and cytoplasmic RNAs from MDA-MB-231 and MCF-7 cells were isolated using a Cytoplasmic and Nuclear RNA Purification Kit (Invitrogen, USA). RT-qPCR was performed to detect the cytoplasmic and nuclear circ_0058063 levels. GAPDH was used as a cytoplasmic control used was as a nuclear control used was U6.

2.6. RNase R treatment

RNase R was applied to circ_0058063 that was extracted from MCF-7 and MDA-MB-231 cells for 30 minutes at 37°C. RT-qPCR was performed to measure RNA levels. Samples without RNase digestion were used as controls.

2.7. CCK-8 assay

Using the Cell Counting Kit-8 test (Biyuntian, Shanghai, China), MCF-7 and MDA-MB-231 cell proliferation viability was examined. In 96-well plates, cells were seeded at a density of 1×10^4 cells/well and cultured for 0, 24, 48, and 72 h. Following incubation, each well received 10 μl of CCK-8 (Dojindo, Kumamoto, Japan), which was then added and cultivated for an additional two hours. The optical density (OD) values at 450 nm in each well were determined using a Multiskan Go Spectrophotometer (Thermo Fisher Scientific, USA).

2.8. Transwell assay

MCF-7 and MDA-MB-231 breast cell migration was assessed using Transwell assays [21]. A total of 5×10^4 cells in a final volume of 100 μL seeded in inserts (24-transwell, Corning, USA) containing 8 μm pores. The

inserts were then placed in wells, and a 600 μL volume of culture medium (DMEM medium supplemented with the 10% FBS) was added. Migrating cells were preserved in 90% methanol for 10 min after 24 h of incubation and then stained for 10 min with 0.1 percent crystal violet. Finally, cells in five randomly selected areas were counted using an Olympus microscope (Olympus, Japan).

2.9. Caspase 3 activity assay

Breast cancer cell apoptosis was investigated using a colorimetric caspase-3 activity assay kit (BioVision Research Products, CA, USA). MCF-7 and MDA-MB-231 cells that had not been transfected or treated were used as blank and unfavorable control samples, respectively. Cells were collected and lysed on ice for 15 min, and the supernatants were collected for further analysis after centrifugation (12,000 $\times$ g for 10 min at 4°C). Each sample was incubated with reaction buffer for two hours. The optical density (OD) was determined at 405 nm using a Multiskan Go Spectrophotometer.

2.10. Xenograft tumor formation assay

All animal experiments were performed in accordance with the Guide for the Care and Use of Laboratory Animals and were approved by the Ethics Committee of our hospital. Six-week-old male nude mice were obtained from our hospital. First, MCF-7 cells stably downexpressing circ_0058063 (Sh-circ) or the corresponding control cells (Sh-NC) were constructed using a recombinant lentivirus expressing the shRNA for circ_0058063 or the control shRNA. The mice were then subcutaneously implanted with 5×10^7 MCF-7 cells in the sh-circ ($n = 5$) or sh-NC ($n = 5$) groups. Using the equation volume = length width2/2, the tumor volume was determined every week. Pentobarbital was injected intravenously to euthanize the mice after five weeks, and the tumors were collected for further investigation.

2.11. Dual-luciferase reporter assays

The circRNA interactome (https://circinteractome.nia.nih.gov) was used to identify the target miRNAs of circ_0058063. To determine the miR-557 target genes, TargetScan (http://www.targetscan.org) was used. The binding interactions between circ_0058063/DLGAP5 and miR-557 were verified using dual-luciferase reporter assays. A firefly luciferase reporter vector (Obio Technology, China) was created by amplification and cloning of the circ_0058063 or DLGAP5 3'UTR sequences. By altering the miR-557 seed region, a mutant variant of the circ_0058063 sequences or the DLGAP5 3'UTR was also produced. Using the Lipofectamine 3000 reagent, we co-transfected either the miR-557 mimic or miR-NC with either wild-type or mutated reporter plasmids. Signals were detected 48 h after transfection, and luciferase activity was estimated by comparing firefly luciferase intensity to that of Renilla luciferase (Obio Technology).

2.12. RNA immunoprecipitation (RIP) assay

A complete RNA immunoprecipitation (RIP) lysis solution (Millipore, USA) with an RNase inhibitor was used to lyse 1×10^7 MCF-7 and MDA-MB-231 cells. The cell extracts were treated with anti-Argonaute 2 (Ago2, #ab32381; Abcam) or anti-IgG antibody (Millipore)-conjugated magnetic beads overnight at 4°C. RIP buffer was used to wash RNA/antibody complexes. TRIzol (Thermo Fisher Scientific, USA) was used to extract RNAs, and qRT-PCR was subsequently performed for further analysis.

2.13. Western blot analysis

Total proteins were isolated using a kit made by KeyGEN (China), called Total Protein Extraction, and protein concentration was evaluated using a BCA kit (Thermo Scientific). RIPA Lysis Buffer (KeyGEN, China) was used to break down 30 g of protein, which was then resolved on a 10% polyacrylamide gel before being blotted onto a PVDF membrane. These membranes were blocked for 1 h in 5% skim milk at 37°C, and then incubated with primary antibodies against DLGAP5 (1:2000, ab70744, Abcam, UK), GAPDH (1:1000, ab8245, Abcam) at 4°C overnight, followed by incubation with the horseradish peroxidase (HRP)-conjugated secondary antibodies (1:50,000, ab6721, Abcam) for 1 h at room temperature. An ECL kit (Clarity Western ECl substrate, Bio-Rad) was used for chemiluminescence detection.

2.14. Statistical analysis

All data in the present study are presented as mean $\pm$ SD. GraphPad Prism version 8 (GraphPad Software, San Diego, CA, USA) was used for all statistical analyses. Student's t-test was used to establish the significance of differences between the two groups. One-way

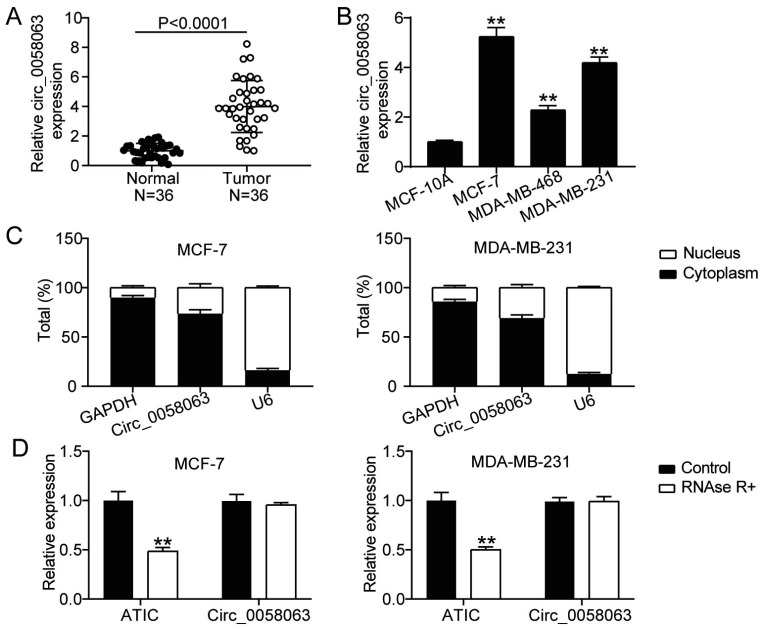

Fig. 1. circ_0058063 was markedly upregulated in BC. (A) circ_0058063 expression study using RT-qPCR in BC and normal tissues. (B) RT-qPCR study of the expression of circ_0058063 in BC cell lines (MCF-7, MDAMB468 and MDAMB231) and in normal BC cell line (MCF10A). $^{**}P < 0.001$ vs. MCF-10A. (C) Subcellular fractionation assay was used to detect subcellular location of circ_0058063 in cytoplasm and nucleus of MDA-MB-231 as well as MCF-7 cells. (D) The existence of circ_0058063 was identified using RNase R. $^{**}P < 0.001$ vs. Control.

ANOVA was used to compare the data from different groups, and Tukey's test was used to analyze the results. Pearson's linear regression analysis was used to analyze the relationship between DLGAP5/miR-557 and circ_0058063/miR-557. The figures and paragraphs include the sample sizes and other statistical parameters. Statistical significance was set at $p < 0.05$.

3. Results

3.1. circ_0058063 was upregulated in BC cells and tissues

RT-qPCR was performed to determine the expression levels of circ_0058063 in BC. The results showed that circ_0058063 expression was considerably increased (four-fold) in cancer tissues compared to normal tissues (Fig. 1A). Additionally, the expression of circ_0058063 was examined in different BC cell lines. According to the RT-qPCR data, circ_0058063 was also clearly upregulated in many BC cell lines (MCF-7, MDA-MB-468, and MDA-MB-231) compared to healthy MCF-10A cells (Fig. 1B). We selected the MDA-MB-231 and MCF-7 cells with the highest circ_0058063 expression for further studies. Considering that cytoplasmic and nuclear circRNAs have different functions, we used a subcellular fractionation test to locate circ_0058063 gene [11]. The results indicated that the predominant locations of circ_0058063 in MCF-7 and MDA-MB-231 cell lines are in the cytoplasm (approximately 80 percent) (Fig. 1C). These results imply that circ_0058063 may serve as a cytoplasmic circRNA and act as a miRNA sponge or an RNA-binding protein scaffold. Finally, to verify the circularity of circ_0058063, an RNase R digestion assay was performed because circRNAs are more resistant to RNase R than linear RNAs. These results indicated that circ_0058063 was resistant to RNase R digestion, whereas linear ATIC was degraded by RNase R digestion (Fig. 1D). These results confirm the presence and strong expression of circ_0058063.

3.2. circ_0058063 promoted BC cell proliferation and migration, while inhibiting cell apoptosis in vitro, and exacerbating tumor growth in vivo

To better understand its role in BC, the expression of circ_0058063 was inhibited in MCF-7 and MDA-MB-231 cells. RT-qPCR was performed to assess the expression level of circ_0058063, and the results indicated that it was down-regulated by approximately 60% in the si-circ group (Fig. 2A). CCK-8, Transwell migration, and caspase 3 activity assays were performed

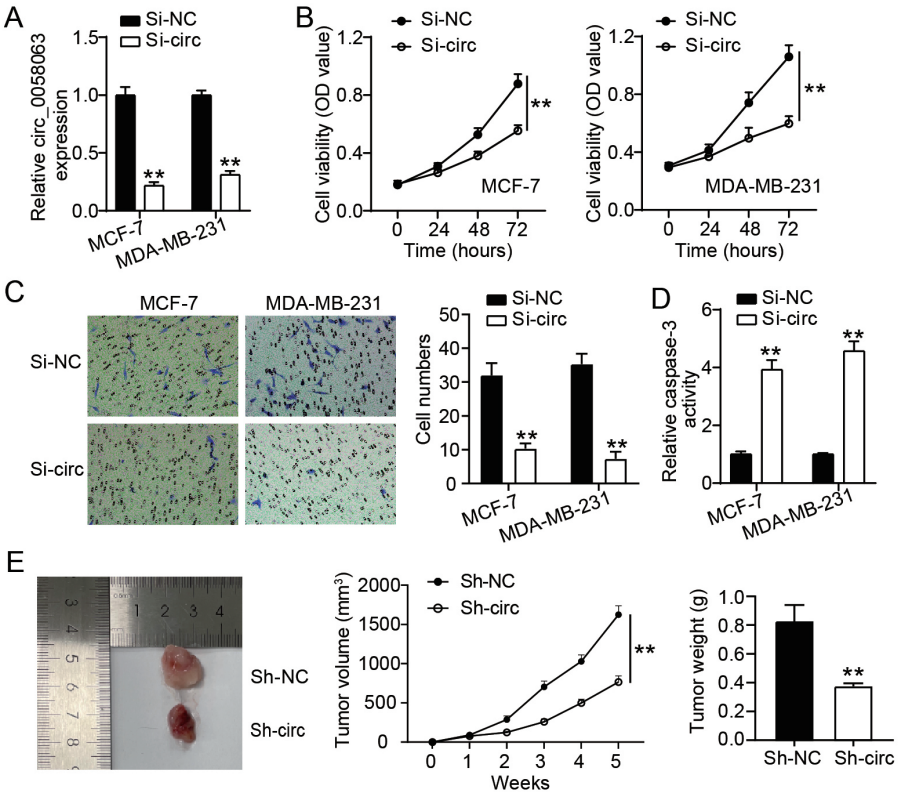

Fig. 2. circ_0058063 downregulation inhibited BC cell growth both *in vitro* and *in vivo*. (A) RT-qPCR study of circ_0058063 expression in MCF-7 and MDA-MB-231 cells after transfection of si-circ_0058063 (si-circ) or si-NC . $^{**}P < 0.001$ vs. Si-NC. (B) The proliferation viability of MDA-MB-231 as well as cells transfected with si-circ or si-NC was assessed using the CCK-8 test. $^{**}P < 0.001$ vs. Si-NC. (C) Transwell assay was performed to detect the migration of MCF-7 and MDA-MB-231 cells transfected with si-circ or si-NC. $^{**}P < 0.001$ vs. Si-NC. (D) Using a capase-3 activity test, the caspase-3 activity of MDA-MB-231 as well as MCF-7 cells transfected with si-circ or si-NC was evaluated. $^{**}P < 0.001$ vs. Si-NC. (E) Nude mice ($n = 5$) received subcutaneous injections of MCF-7 cells stably transfected with sh-control (sh-NC) or sh-circ into the right flank. A one-time weekly measurement of xenograft tumor volumes was performed during treatment, and xenograft tumors were photographed on 5 weeks after each mouse was sacrificed. $^{**}P < 0.001$ vs. sh-NC.

to investigate the effects of circ_0058063 on MCF-7 and MDA-MB-231 cell growth. The CCK-8 assay demonstrated that silencing circ_0058063 dramatically reduced the viability of MCF-7 and MDA-MB-231 cells (Fig. 2B). Moreover, Transwell assays showed that circ_0058063 silencing prevented the migration of MDA-MB-231 and MCF-7 cells (Fig. 2C). These experiments demonstrated that circ_0058063 promotes the proliferation and migration of BC cells. Interestingly, we also noted that circ_0058063 knockdown exhibited enhanced caspase 3 activity indicating that the inhibition of circ_0058063 promotes BC cell apoptosis (Fig. 2D). Finally, a mouse xenograft model with circ_0058063 knockdown in primary MCF-7 cells was constructed to assess the effect of circ_0058063 on BC cell proliferation *in vivo*. Consistent with the *in vitro* results, the knockdown of circ_0058063 led to a reduction in tumor weight and growth (Fig. 2E). These findings suggested that circ_0058063 regulates BC development in an oncogenic manner.

3.3. circ_0058063 acted as a sponge for miR-557

Previous studies have reported that circ_0058063 serves as a cytoplasmic circRNA that acts as a sponge for miRNA. Therefore, to determine the probable targets of circ_0058063, we employed a circular RNA interactome (https://circinteractome.nia.nih.gov). We speculated that miR-557 may be a potential target of circ_0058063. Two potential binding sites were predicted between circ_0058063 and miR-557 using the circRNA interactome (Fig. 3A). To verify these binding sites, a luciferase activity assay was performed by constructing wild-type circ_0058063 and mutant circ_0058063 vectors (binding site 1 mutant, binding site 2 mutant, and binding site 1/2 co-mutant). We

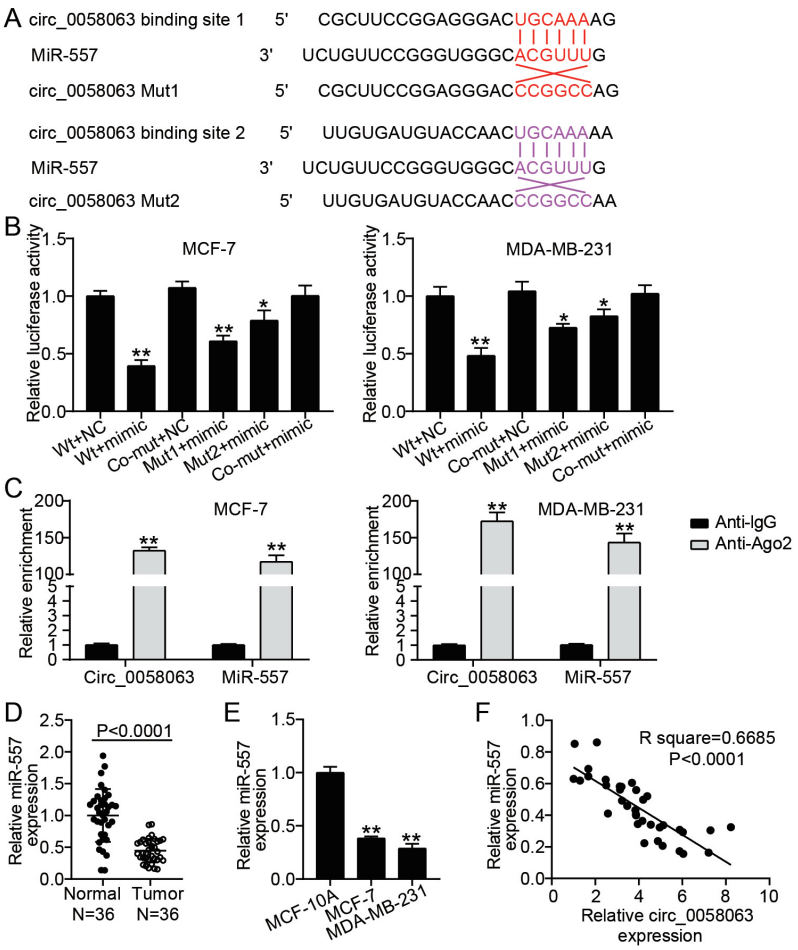

Fig. 3. miR-557 was a target of circ_0058063. (A) The binding sites among miR-557 and circ_0058063 were anticipated by circRNA interactome. (B) The relationship between miR-557 and circ_0058063 was confirmed by dual-luciferase reporter assay in MDA-MB-231 as well as MCF-7 cells. $^{**}P < 0.001$ vs. Wt+NC. (C) The relationship between miR-557 and circ_0058063 was confirmed by RIP assay in MCF-7 and MDA-MB-231 cells. $^{**}P < 0.001$ vs. Anti-IgG. (D) RT-qPCR analysis of miR-557 expressions in BC and normal tissues. (E) RT-qPCR analysis of miR-557 expressions in normal breast cell lines (MCF-10A) and BC cell lines (MCF-7 and MDA-MB-231). $^{**}P < 0.001$ vs. MCF-10A. (F) RT-qPCR analyzed the association between circ_0058063 and miR-557 in BC tissues (Pearson linear regression analysis).

noted that the miR-557 mimic significantly reduced the relative circ_0058063 luciferase activity in the wild-type, binding site 1 mutant, and binding site 2 mutant circ_0058063 cells; however, there was no change in the co-mutant circ_0058063 cells (Fig. 3B). These data indicate that circ_0058063 may bind to miR-557. To support this claim regarding the binding relationship between circ_0058063 and miR-557 in MDA-MB-231 and MCF-7 cells, RIP was performed. The anti-AGO2 RIP assay results showed that miR-557 mimic transfection increased the amount of circ_0058063 in RNAs enriched for AGO2 (Fig. 3C), suggesting that miR-557 interacts with circ_0058063 in MCF-7 and MDA-MB-231 cells. Next, we determined the level of miR-557 in BC cell lines using RT-qPCR. The results revealed that miR-557 was downregulated in BC tissues (Fig. 3D) and cells (Fig. 3E) and had a negative linear correlation with circ_0058063 expression levels in BC tissues (Fig. 3F). These results revealed that circ_0058063 controls miR-557 expression by serving as an miRNA sponge.

3.4. *circ_0058063 facilitated the proliferation and migration of BC cells while suppressing cell apoptosis by targeting miR-557*

We tested whether miR-557 knockdown could undo the impact of circ_0058063 knockdown in BC cells to further support the hypothesis that circ_0058063 serves as a sponge for miR-557. According to the PCR data,

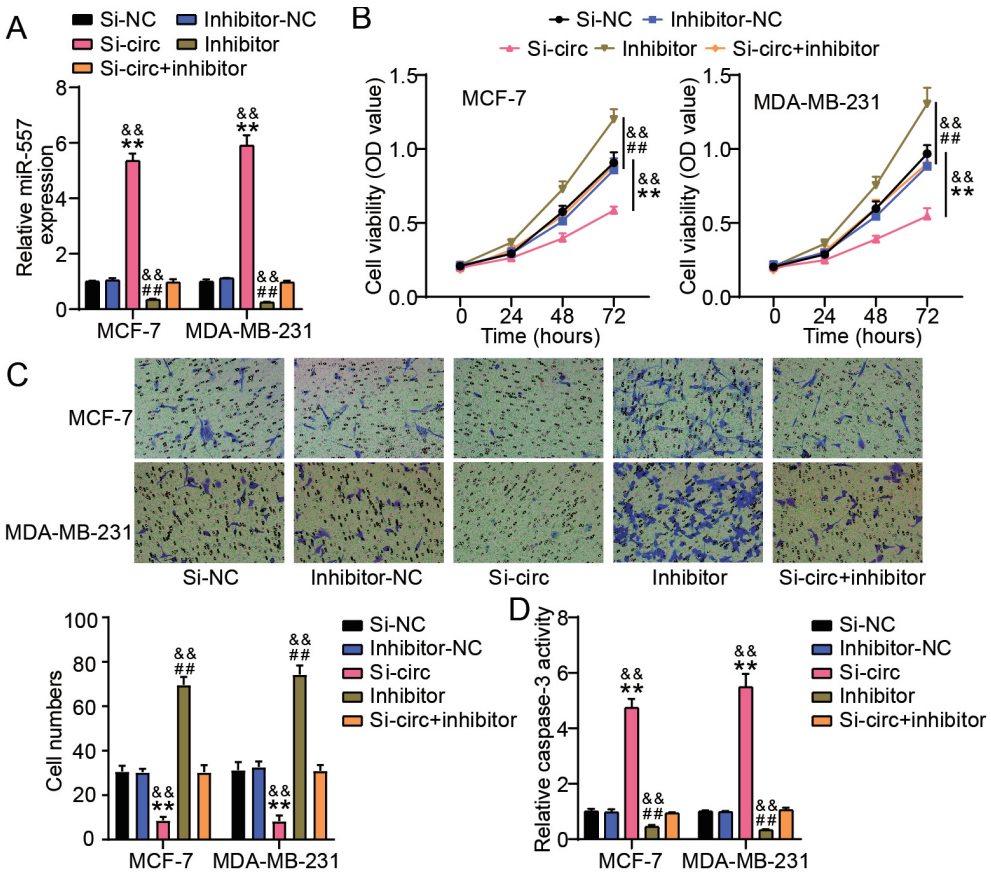

Fig. 4. circ_0058063 facilitated the migration and proliferation of BC cells while suppressed cell apoptosis by targeting miR-557. (A) RT-qPCR analysis of miR-557 expressions in MCF-7 and MDA-MB-231 cells after transfection of si-NC, si-circ, miR-557 inhibitor (inhibitor), inhibitor-NC or si-circ+inhibitor. (B) The proliferation viablity of these transfected MCF-7 and MDA-MB231 cells was assessed using the CCK-8 test. (C) These previously stated transfected MCF-7 and MDA-MB-231 cells underwent a transwell experiment to assess their migration. (D) Levels of caspase-3 of these above-mentioned transfected MDA-MB-231 as well as MCF-7 cells were examined using capase-3 activity assay. $^{\#\#}P <$ 0.001 vs. inhibitor-NC; $^{**}P < 0.001$ vs. Si-NC; $^{\&\&}P < 0.001$ vs. Si-circ+inhibitor.

miR-557 was considerably increased by the knockdown of circ_0058063, whereas it was strongly downregulated by the miR-557 inhibitor in both MDA-MB-231 and MCF-7 cells (Fig. 4A). Using functional assays, we found that miR-557 knockdown considerably aided MDA-MB-231 and MCF-7 cell growth (Fig. 4B). Although the knockdown of circ_0058063 inhibited BC cell proliferation, this effect was reversed when miR-557 expression was inhibited (Fig. 4B). Additionally, the Transwell assay in MDA-MB-231 and MCF-7 cells showed that the number of migrated cells was lower in the si-circ_0058063 + miR-557 inhibitor group than in the miR-557 inhibitor group (Fig. 4C). We also noted that the knockdown of miR-557 impaired the effect of circ_0058063 knockdown on BC cell apoptosis (Fig. 4D). These findings suggested that miR-557 knockdown reduced the effects of circ_0058063 knockdown on BC cell proliferation, migration, and apoptosis.

3.5. *DLGAP5 served as the functional protein of miR-557*

Next, we explored the downstream target genes of miR-557. TargetScan (https://www.targetscan.org/vert_71/) indicated that miR-557 had complementary sites in DLGAP5 mRNA-3'UTR (Fig. 5A). Overexpression of miR-557 decreased wild-type DLGAP5 activity but not mutant DLGAP5 activity, according to the luciferase activity test (Fig. 5B). These findings suggested that miR-557 mayspecifically target 3'UTR of DLGAP5. RT-qPCR analysis also showed that DLGAP5 mRNA levels were significantly upregulated in both BC cells (5 folds) (Fig. 5C) and tissues (5 folds) (Fig. 5D). More-

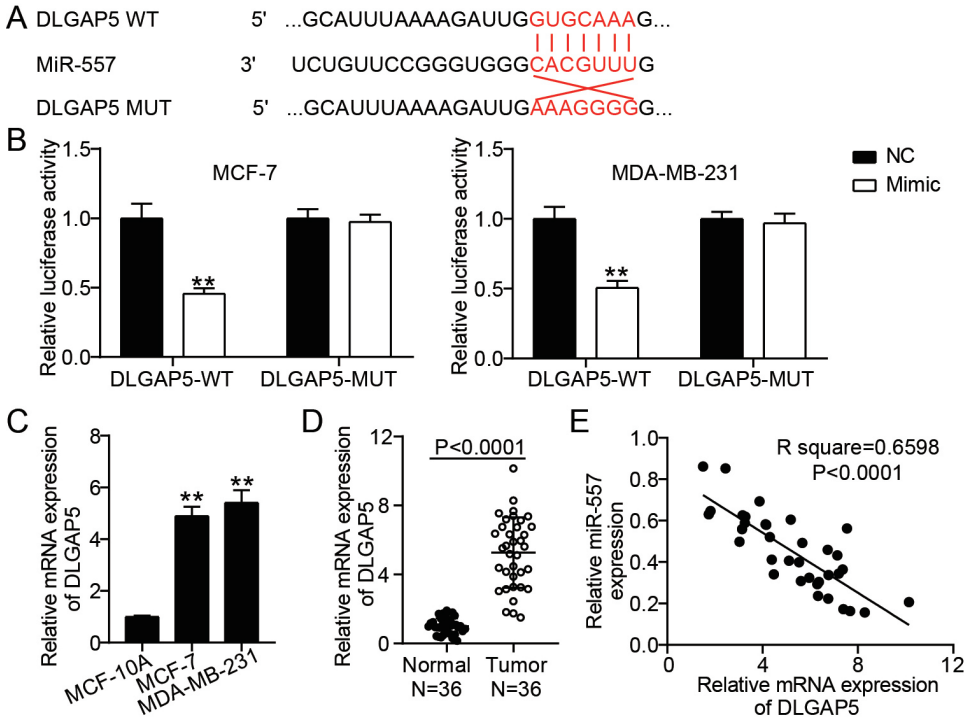

Fig. 5. DLGAP5 was a target of miR-557 (A) TargetScan made predictions about the miR-557 and DLGAP5 binding locations. (B) The relationship among miR-557 and DLGAP5 was confirmed by dual-luciferase reporter assay in MDA-MB-231 as well as MCF-7 cells. $^{**}P < 0.001$ vs. NC. (C) RT-qPCR analysis of DLGAP5 expressions in normal breast cell lines (MCF-10A) and BC cell lines (MCF-7 and MDA-MB-231). $^{**}P < 0.001$ vs. MCF-10A. (D) DLGAP5 expression in BC and normal tissues was analyzed using RT-qPCR. (E) The association between miR-557 and DLGAP5 in BC tissues was examined using RT-qPCR (Pearson linear regression analysis).

over, DLGAP5 expression showed a negative linear correlation with the expression level of miR-557 (Fig. 5E). These results suggest that DLGAP5 serves as a downstream target of miR-557.

3.6. miR-557 repressed the proliferation and migration of BC cells while suppressing cell apoptosis by downregulating DLGAP5 expression

To confirm whether DLGAP5 acts as a target of miR-557, we evaluated whether DLGAP5 knockdown could reverse the effects of miR-557 silencing in BC cells. The results showed that transfection with si-DLGAP5 significantly reduced DLGAP5 expression, whereas miR-557 downregulation significantly upregulated the expression of DLGAP5 both in MDA-MB-231 and MCF-7 cells (Fig. 6A). Although DLGAP5 knockdown inhibited BC cell proliferation, this effect was reversed when miR-557 expression was inhibited (Fig. 6B). Additionally, the Transwell assay revealed fewer migrating cells in the si-DLGAP5 + miR-557 inhibitor group than in the miR-557 inhibitor group, indicating that the additional miR-557 inhibitor eliminated the ability of DLGAP5 to restrict migration in BC cells. (Fig. 6C). Furthermore, we observed that in both MCF-7 and MDA-MB-231 cells, the reduction of miR-557 expression reduced the facilitation effects of DLGAP5 knockdown on cell apoptosis (Fig. 6D). These results showed that miR-557 knockdown alleviated the effect of DLGAP5 knockdown on the proliferation, migration, and apoptosis of BC cells.

4. Discussion

The high incidence of BC constitutes a serious threat to the health of women, because it is the most prevalent cancer worldwide [1,2]. Although significant efforts have been made to reduce mortality, the exact mechanisms underlying the initiation and progression of BC remain elusive [3,22]. circ_0058063 expression is enhanced in BC. circ_0058063 knockdown prevents BC cells from proliferating and migrating, while inducing cell death. Mechanistically, circ_0058063 acted as a sponge for miR-557 to upregulate DLGAP5 expression, and knockdown of DLGAP5 significantly inhibited BC

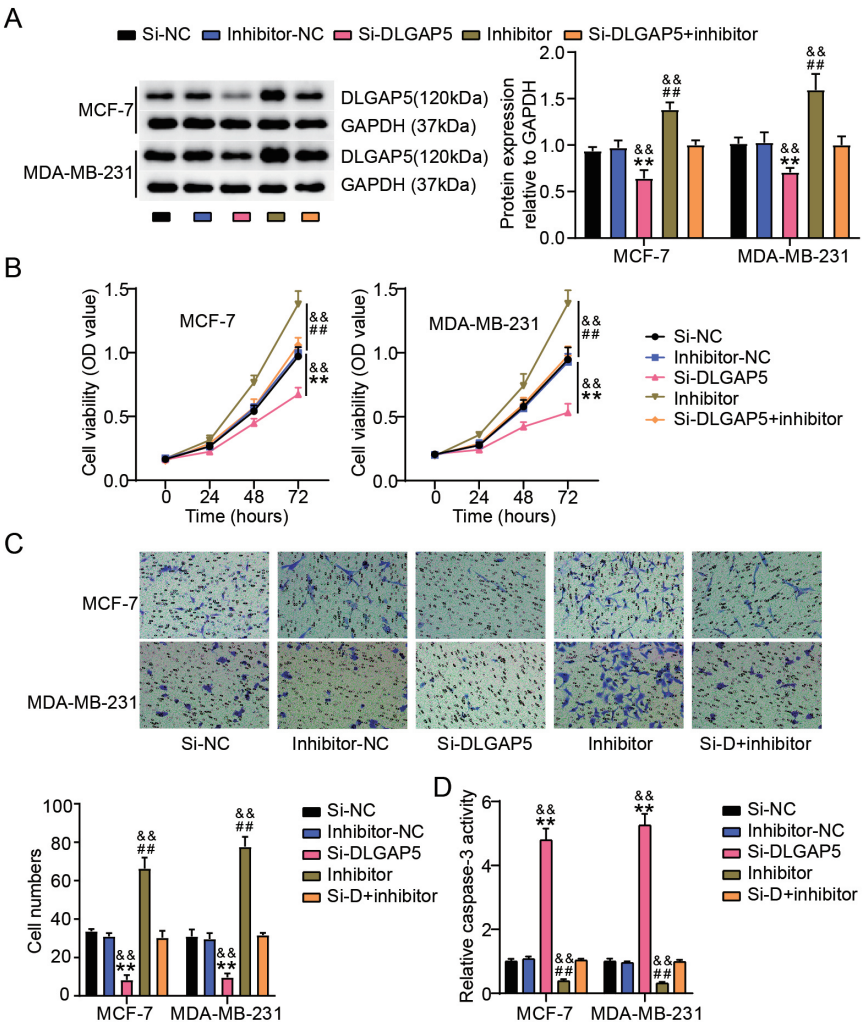

Fig. 6. miR-557 repressed the proliferation and migration of BC cells while suppressed cell apoptosis by downregulating DLGAP5 expression. (A) Results of western blot study of DLGAP5 expressions in MDA-MB-231 as well as MCF-7 cells after transfection of si-NC, si-DLGAP5, miR-557 inhibitor (inhibitor), inhibitor-NC or si-DLGAP5+inhibitor. (B) To quantify the proliferation of these transfected MDA-MB-231 cells as well as MCF-7, the CCK-8 test was used. (C) To monitor the migration of these transfected MDA-MB-231 and MCF-7 cells, a transwell test was performed. (D) Employing a capase-3 activity test, caspase-3 levels in these transfected MDA-MB-231 as well as MCF-7 cells were evaluated. $^{\#\#}P < 0.001$ vs. inhibitor-NC; $^{**}P < 0.001$ vs. Si-NC; $^{\&\&}P < 0.001$ vs. Si-DLGAP5+inhibitor. Si-DLGAP5: Si-D.

cell survival. Overall, circ_0058063 is a novel circRNA that regulates BC progression.

Recent studies have demonstrated an association between circRNAs and various cancers [12,23]. CircRNAs have been implicated in the progression of BC through migration and regulation of cancer cell proliferation, invasion, and metastasis [23–25]. We identified circ_0058063 as a novel circRNA involved in the regulation of BC progression. Previous studies have reported that circ_0058063 is also upregulated in other types of cancers, including multiple myeloma, esophageal squamous cell carcinoma, and bladder cancer [19,26–28]. In detail, circ_0058063 promotes cancer cell proliferation and invasion and inhibits apoptosis in multiple myeloma and bladder cancer, which is consistent with our results [19,26,27]. Our results in the present study demonstrated that circ_0058063 is abnormally highly expressed in BC cells. Moreover, circ_0058063 knockdown inhibited BC cell growth *in vitro* and *in vivo*. Mechanistically, circ_0058063 plays an essential role in regulating cellular metabolism and GLUT1 expression, which can increase glucose uptake in cancer cells to promote cell proliferation [27]. These findings suggest that circ_0058063 is a useful cancer biomarker for both diagnosis and treatment.

circRNAs regulate cancer progression through various biological effects and mechanisms [9,29]. Many circRNAs serve as miRNAs or protein inhibitors ('sponges') that regulate protein functions [29]. Circ _0058063 acts as a molecular sponge for miRNAs, regulating the expression of its target genes to influence cell growth and death [19,26]. For instance, miR-635 is targeted and negatively regulated by circ_0058063 in multiple myeloma (MM), and miR-635 knockdown reduces the effects of circ_0058063 on the migration, proliferation, and invasion of MM cells [26]. By sponging miR-486-3p, circ_0058063 promotes rapid growth of bladder cancer [28]. In this study, we demonstrate that miR-557 is a novel target of circ_0058063 in BC. miR-557 is an anti-tumor miRNA that plays a profound role in the formation and development of a number of malignancies, such as osteosarcoma, pancreatic cancer, and lung cancer [30–33]. Overexpression of miR-557 targets SLC7A11, which is closely linked to the emergence of many malignant tumors and reduces the malignant potential of pancreatic cancer cells. miR-557 is downregulated in pancreatic cancer cells [31]. We also observed that miR-557 was downregulated in BC cells and that miR-557 knockdown reversed the inhibitory effect of circ_0058063 knockdown on BC proliferation and migration. These results also showed that miR-557 is a target of circ_0058063, which affects BC progression.

Subsequently, we demonstrated that DLGAP5 was a target of miR-557. Unlike other DLGAP family members, DLGAP5 is mainly associated with various types of cancers [34]. DLGAP5 promotes microtubule polymerization and bipolar spindle formation, which facilitates mitosis by passing through the G2/M checkpoint [35,36]. Numerous malignancies, including hepatocellular carcinoma, lung cancer, ovarian cancer, gliomas, and pancreatic cancer, have been shown to have elevated levels of DLGAP5 [37–39]. According to previous studies, DLGAP5 is considerably elevated in BC tissues and is linked with tumor grade and lymph node status [40,41]. Higher DLGAP5 expression is associated with poor prognosis [41]. Consistent with previous studies, we demonstrated that DLGAP5 was upregulated and participated in the regulation of BC cell proliferation. In mechanism, knockdown of DLGAP5 significantly downregulated the expression of cell cycle-related proteins, CDK1, Cyclin B1, induced G2/M phase arrest, and inhibited cell proliferation [37]. Furthermore, DLGAP5 upregulates the expression of Bcl-2 and downregulates Bax expression, which can inhibit cell apoptosis [19]. As DLGAP5 exhibits an isolated microtubule-associated protein 1A/1B light chain 3B-interacting region motif and is located in the mitochondria, recent studies have shown that DLGAP5 may play a role in mitophagy [41]. These studies showed that DLGAP5 plays a vital role in cancer progression and may serve as a candidate target for the diagnosis and treatment of BC. Furthermore, DLGAP5 was found to be a target of miR-557, which reversed the antitumor effects of miR-557 on BC cell growth. In summary, DLGAP5 facilitated BC progression and was targeted by miR-556-5p.

This study has some limitations. First, the correlation between aberrant circ_0058063 expression levels and the clinicopathological characteristics of patients with BC has not been fully analyzed. Second, whether there is a correlation between driver oncogene mutation type and circ_0058063 expression in BC remains to be explored. We intend to address these questions in future studies. In addition, owing to the key regulatory effect of abnormal circ_0058063 expression in BC, whether circ_0058063 with high and low expression is correlated with the prognosis of BC should be explored in the future by collecting more clinical samples.

5. Conclusion

Our study showed that miR-557 expression was decreased in BC, while circ_0058063 expression was increased. circ_0058063 knockdown significantly reduced BC cell proliferation and migration. Mechanistically, circ_0058063 targets miR-557, which downregulates DLGAP5. Our findings regarding the circ_005806 3/miR-557/DLGAP5 axis may provide a potential target for BC therapy and early diagnosis.

Funding

There was no funding received.

Conflict of interest

There were no conflicts of interest, according to the authors.

Ethics approval

The Ethics Committee of Wuhan NO.1 Hospital (Wuhan, China) approved this study. The processing

of the clinical tissue samples complied with the ethical principles of the Declaration of Helsinki. All of the patients completed an informed consent form.

The animal experiment conducted observed the ARRIVE guidelines and was authorized by the Ethics Committee of Wuhan NO.1 Hospital (Wuhan, China).

Consent to participate

All patients signed a written informed consent.

Consent for publication

The participants gave their consent for the study to be published.

Availability of data and material

This article contains all of the data that were created or examined during this investigation.

Authors' contributions

Conception: CMT.
Interpretation or analysis of data: KJZ and CY.
Preparation of the manuscript: CMT and CY.
Revision for important intellectual content: KJZ.
Supervision: CY.
The article has been reviewed and approved by all authors.

Acknowledgments

None.

References

[1] Y. Shieh and J.A. Tice, Medications for Primary Prevention of Breast Cancer, *Jama* **324** (2020), 291–292.
[2] S. Loibl, P. Poortmans, M. Morrow, C. Denkert and G. Curigliano, Breast cancer, *Lancet* **397** (2021), 1750–1769.
[3] K.L. Britt, J. Cuzick and K.A. Phillips, Key steps for effective breast cancer prevention, *Nat Rev Cancer* **20** (2020), 417–436.
[4] A.G. Waks and E.P. Winer, Breast Cancer Treatment: A Review, *JAMA* **321** (2019), 288–300.
[5] M. Berdasco and M. Esteller, Clinical epigenetics: seizing opportunities for translation, *Nat Rev Genet* **20** (2019), 109–127.
[6] B.G. Haffty, D.M. Euhus and L.J. Pierce, Genetic Factors in the Locoregional Management of Breast Cancer, *J Clin Oncol* **38** (2020), 2220–2229.
[7] L. Garcia-Martinez, Y. Zhang, Y. Nakata, H.L. Chan and L. Morey, Epigenetic mechanisms in breast cancer therapy and resistance, *Nat Commun* **12** (2021), 1786.
[8] L.L. Chen, The expanding regulatory mechanisms and cellular functions of circular RNAs, *Nat Rev Mol Cell Biol* **21** (2020), 475–490.
[9] L.S. Kristensen, M.S. Andersen, L.V.W. Stagsted, K.K. Ebbesen, T.B. Hansen and J. Kjems, The biogenesis, biology and characterization of circular RNAs, *Nat Rev Genet* **20** (2019), 675–691.
[10] S. Aufiero, Y.J. Reckman, Y.M. Pinto and E.E. Creemers, Circular RNAs open a new chapter in cardiovascular biology, *Nat Rev Cardiol* **16** (2019), 503–514.
[11] A.J. van Zonneveld, M. Kölling, R. Bijkerk and J.M. Lorenzen, Circular RNAs in kidney disease and cancer, *Nat Rev Nephrol* **17**(12) (2021), 814–826.
[12] G.J. Goodall and V.O. Wickramasinghe, RNA in cancer, *Nat Rev Cancer* **21** (2021), 22–36.
[13] L. He, C. Man, S. Xiang, L. Yao, X. Wang and Y. Fan, Circular RNAs' cap-independent translation protein and its roles in carcinomas, *Mol Cancer* **20** (2021), 119.
[14] H. Shen, B. Liu, J. Xu, B. Zhang, Y. Wang, L. Shi and X. Cai, Circular RNAs: characteristics, biogenesis, mechanisms and functions in liver cancer, *J Hematol Oncol* **14** (2021), 134.
[15] J. Li, Y. Li and H. Cheng, Circ-RPPH1 knockdown retards breast cancer progression via miR-328-3p-mediated suppression of HMGA2, *Clin Breast Cancer* **22**(3) (2021), e286–e295.
[16] L. Li, G. Feng, T. Chen and L. Zhang, Circ_0000514 promotes breast cancer progression by regulating the miR-296-5p/CXCL10 axis, *J Biochem* **170**(6) (2021), 753–761.
[17] B. Fu, W. Liu, C. Zhu, P. Li, L. Wang, L. Pan, K. Li, P. Cai, M. Meng, Y. Wang, A. Zhang, W. Tang and M. An, Circular RNA circBCBM1 promotes breast cancer brain metastasis by modulating miR-125a/BRD4 axis, *Int J Biol Sci* **17** (2021), 3104–3117.
[18] Z.G. Chen, H.J. Zhao, L. Lin, J.B. Liu, J.Z. Bai and G.S. Wang, Circular RNA CirCHIPK3 promotes cell proliferation and invasion of breast cancer by sponging miR-193a/HMGB1/PI3K/AKT axis, *Thorac Cancer* **11** (2020), 2660–2671.
[19] M. Sun, W. Zhao, Z. Chen, M. Li, S. Li, B. Wu and R. Bu, Circ_0058063 regulates CDK6 to promote bladder cancer progression by sponging miR-145-5p, *J Cell Physiol* **234** (2019), 4812–4824.
[20] M. Tang, F. Wang, K. Wang, Y. Jiang and Q. Wang, Circ_0058063 promotes progression of thyroid cancer by sponging miR-330-3p/SDC4 axis, *Anticancer Drugs* **33** (2022), 642–651.
[21] C. Chen, P. Gupta, D. Parashar, G.G. Nair, J. George, A. Geethadevi, W. Wang, S.W. Tsaih, W. Bradley, R. Ramchandran, J.S. Rader, P. Chaluvally-Raghavan and S. Pradeep, ERBB3-induced furin promotes the progression and metastasis of ovarian cancer via the IGF1R/STAT3 signaling axis, *Oncogene* **39** (2020), 2921–2933.
[22] N. Harbeck, F. Penault-Llorca, J. Cortes, M. Gnant, N. Houssami, P. Poortmans, K. Ruddy, J. Tsang and F. Cardoso, Breast cancer, *Nat Rev Dis Primers* **5** (2019), 66.
[23] T. Tian, Y. Zhao, J. Zheng, S. Jin, Z. Liu and T. Wang, Circular RNA: A potential diagnostic, prognostic, and therapeutic biomarker for human triple-negative breast cancer, *Mol Ther Nucleic Acids* **26** (2021), 63–80.
[24] M. Zhang, X. Bai, X. Zeng, J. Liu, F. Liu and Z. Zhang, circRNA-miRNA-mRNA in breast cancer, *Clin Chim Acta* **523** (2021), 120–130.
[25] S. Ghafouri-Fard, B.M. Hussen, M. Taheri and S.A. Ayatollahi,

Emerging role of circular RNAs in breast cancer, *Pathol Res Pract* **223** (2021), 153496.

[26] X. Li, L. Ding, G. Gu, C. Zheng, C. Pan, Q. Zheng and T. Xiang, Role and Mechanism of circ_0058063/miR-635 Axis in the Malignant Phenotype of Multiple Myeloma RPMI8226 Cells, *Evid Based Complement Alternat Med* **2021** (2021), 4630934.

[27] Y. Zheng, Y. Chen, H. Jiang, H. Zhang, H. Wang, J. Xu and Z. Yu, Circ_0058063 upregulates GLUT1 expression and promotes glucose-uptake in esophageal squamous-cell carcinomas, *J Thorac Dis* **12** (2020), 925–931.

[28] H. Liang, H. Huang, Y. Li, Y. Lu and T. Ye, CircRNA_0058063 functions as a ceRNA in bladder cancer progression via targeting miR-486-3p/FOXP4 axis, *Biosci Rep* **40** (2020), BSR20193484.

[29] L. Szabo and J. Salzman, Detecting circular RNAs: bioinformatic and experimental challenges, *Nat Rev Genet* **17** (2016), 679–692.

[30] Y. Wang, W. Hao and H. Wang, miR-557 suppressed the malignant behaviours of osteosarcoma cells by reducing HOXB9 and deactivating the EMT process, *Artif Cells Nanomed Biotechnol* **49** (2021), 230–239.

[31] T. Zhang, M. Li, H. Lu and T. Peng, Up-Regulation of circEIF6 Contributes to Pancreatic Cancer Development Through Targeting miR-557/SLC7A11/PI3K/AKT Signaling, *Cancer Manag Res* **13** (2021), 247–258.

[32] Y. Yang, K.K. Sun, X.J. Shen, X.Y. Wu and D.C. Li, miR-557 inhibits the proliferation and invasion of pancreatic cancer cells by targeting EGFR, *Int J Clin Exp Pathol* **12** (2019), 1333–1341.

[33] J. Qiu, Y. Hao, S. Huang, Y. Ma, X. Li, D. Li and Y. Mao, MiR-557 works as a tumor suppressor in human lung cancers by negatively regulating LEF1 expression, *Tumour Biol* **39** (2017), 1010428317709467.

[34] A.H. Rasmussen, H.B. Rasmussen and A. Silahtaroglu, The DLGAP family: neuronal expression, function and role in brain disorders, *Mol Brain* **10** (2017), 43.

[35] J. Wong and G. Fang, HURP controls spindle dynamics to promote proper interkinetochore tension and efficient kinetochore capture, *J Cell Biol* **173** (2006), 879–91.

[36] R. Zheng, Z. Shi, W. Li, J. Yu, Y. Wang and Q. Zhou, Identification and prognostic value of DLGAP5 in endometrial cancer, *PeerJ* **8** (2020), e10433.

[37] H. Zhang, Y. Liu, S. Tang, X. Qin, L. Li, J. Zhou, J. Zhang and B. Liu, Knockdown of DLGAP5 suppresses cell proliferation, induces G(2)/M phase arrest and apoptosis in ovarian cancer, *Exp Ther Med* **22** (2021), 1245.

[38] D. Zhou, M. Wang, Y. Zhang, K. Wang, M. Zhao, Y. Wang, X. Wang, R. Yu and X. Zhou, Screening and identification of LMNB1 and DLGAP5, two key biomarkers in gliomas, *Biosci Rep* **41** (2021), BSR20210231.

[39] M.J. Ke, L.D. Ji and Y.X. Li, Bioinformatics analysis combined with experiments to explore potential prognostic factors for pancreatic cancer, *Cancer Cell Int* **20** (2020), 382.

[40] Y. Weng, W. Liang, Y. Ji, Z. Li, R. Jia, Y. Liang, P. Ning and Y. Xu, Key Genes and Prognostic Analysis in HER2+ Breast Cancer, *Technol Cancer Res Treat* **20** (2021), 1533033820983298.

[41] T. Xu, M. Dong, H. Li, R. Zhang and X. Li, Elevated mRNA expression levels of DLGAP5 are associated with poor prognosis in breast cancer, *Oncol Lett* **19** (2020), 4053–4065.